MECHANIKA TEORETYCZNA
I STOSOWANA
Journal of Theoretical
and Applied Mechanics
2, 35, 1997

AN h-ADAPTIVE FINITE ELEMENT METHOD FOR NAVIER-STOKES EQUATIONS

WALDEMAR RACHOWICZ

Section of Applied Mathematics, Technical University of Cracow

e-mail: waldek@oeto.pk.edu.pl

Application of an h-adaptive finite element method to incompressible Navier-Stokes equations in two dimensions is presented. Projection methods (pressure correction methods) due to A. Chorin are used to discretize the problem in time. Triangular elements of the order $p = 1$ and $p = 2$ are used in spatial discretization. The method of 1-irregular meshes and the Rivara technique are used to generate adaptive meshes. A mesh-refinement strategy is based on residual error indicators due to Oden, Wu and Ainsworth.

Key words: Navier-Stokes equations, adaptive finite element method, a posteriori error estimates

1. Motivation

The idea of adaptivity in numerical analysis expresses a very intuitive concept of enriching the discretization selectively in the regions, where the approximate solution is essentially less accurate than in the rest of computational domain. Thus it is expected to improve the solution with least computational effort. The efficiency of such a procedure is observed especially if solutions are significantly irregular. This makes approximations of flow problems very likely candidates for applying adaptive methods, as their solutions are characterized by irregularities like point singularities, boundary and internal layers (shocks).

A quantitative assessment of advantages resulting from adaptivity in the finite element method can be illustrated in terms of an idealized problem of interpolation. The arguments presented below were originated by Babuška and Rheinboldt (1978).

We consider a construction of a non-uniform finite element mesh which would be optimal in a sense of minimizing the interpolation error for a fixed number of elements. For rectangular elements with bilinear approximation the interpolation error in the H^1-seminorm can be estimated as:

$$|u - u_I|^2_{1,K} \leq C h_K^2 \int_K (u^2_{,xx} + u^2_{,yy})\, dx \tag{1.1}$$

where

u_I – interpolant of u

h_K – element size.

We will minimize the sum of the expressions on the right-hand side of Eq (1.1) with the restriction that the number of elements is N_a. That is instead of the true error, which is a hard to compute quantity, we will rather deal with an expression which bounds the error (still, for simplicity, calling it "error"). Assuming that $h(\boldsymbol{x})$ is an unknown (piecewise constant) function we formulate the following minimization problem:

find $h(\boldsymbol{x})$ such that

$$\begin{aligned} &\int_\Omega h(\boldsymbol{x})^2 (u^2_{,xx} + u^2_{,yy})\, dx \equiv e^2 = \min \\ &\int_\Omega \frac{dx}{h^2(x)} = N_a \end{aligned} \tag{1.2}$$

The last integral in Eqs (1.2) represents the number of elements and e denotes the total error. We use the standard Lagrange multiplier method to solve the problem

$$\int_\Omega 2h(u^2_{,xx} + u^2_{,yy})\delta h\, dx - \lambda \int_\Omega 2\frac{dx}{h^3}\delta h = 0 \qquad \forall \delta h \tag{1.3}$$

which implies the optimality criterion for $h(\boldsymbol{x})$

$$h^4(u^2_{,xx} + u^2_{,yy}) = \lambda \tag{1.4}$$

This characterization can be reinterpreted in view of the fact that $h(\boldsymbol{x})$ must be a piecewise constant function and that derivatives of $u(\boldsymbol{x})$ vary insignificantly, if elements are small, resulting in the condition

$$h_K^2 \int_K (u^2_{,xx} + u^2_{,yy})\, dx = \lambda \tag{1.5}$$

Criterion (1.5) is referred to as *the equidistribution of errors principle* for optimal meshes. It provides the justification for the intuitive adaptive strategy saying: "break elements with the biggest errors", as such a procedure leads to the equidistribution of errors. Eqs $(1.2)_1$ and (1.5) indicate that $\lambda = e^2/N_a$. Thus expressing $h(\boldsymbol{x})$ from Eq (1.4), $h(\boldsymbol{x}) = \sqrt[4]{e^2/[N_a(u^2_{,xx} + u^2_{,yy})]}$, and introducing it to Eqs (1.2) we obtain the relation between e and N_a

$$N_a = \frac{1}{e^2}\Big(\int\limits_{\Omega} \sqrt{u^2_{,xx} + u^2_{,yy}}\, dx\Big)^2 \tag{1.6}$$

An analogous relation between the number of elements N_u and the error for uniform meshes is obtained by noting that

$$e^2 = h^2 \int\limits_{\Omega} (u^2_{,xx} + u^2_{,yy})\, dx \tag{1.7}$$

and $h^2 = S/N_u$, where $S = meas(\Omega)$. Therefore we have

$$N_u = \frac{1}{e^2} S \int\limits_{\Omega} (u^2_{,xx} + u^2_{,yy})\, dx \tag{1.8}$$

An elementary use of the Cauchy-Schwarz inequality

$$\Big(\int\limits_{\Omega} \sqrt{u^2_{,xx} + u_{,yy}} \cdot 1 dx\Big)^2 \leq \int\limits_{\Omega} (u^2_{,xx} + u^2_{,yy})\, dx \cdot \int\limits_{\Omega} 1\, dx \tag{1.9}$$

shows that, in view of Eqs (1.7) and (1.8)

$$N_a \leq N_u \tag{1.10}$$

which proves the expected superiority of adaptive meshes over uniform meshes. To illustrate the savings resulting from application of optimal meshes we consider a model function with an internal boundary layer

$$u(\boldsymbol{x}) = \arctan[a(r - r_0)] \qquad \boldsymbol{x} \in \Omega \equiv [0,1]^2 \tag{1.11}$$

where $r = \sqrt{x^2 + y^2}$, $r_0 = 1/2$, a is a parameter that controls irregularity of $u(\boldsymbol{x})$. Table 1 shows the savings factor N_u/N_a for various values of parameter a. We observe that N_u/N_a grows to spectacular values as $u(\boldsymbol{x})$ becomes more irregular. These results indicate overwhelmingly that for some classes of problems the use of adaptivity becomes simply an inevitable necessity rather than just a more elegant way of solving the problem.

Table 1. The dependence of the savings factor on irregularity of the interpolated function

a	N_u/N_a
5	1.65
10	2.67
20	5.11
40	10.16

The arguments presented above are very strong motivation to apply an adaptive finite element method to computational fluid dynamics. In this work we present application of adaptivity to solving the incompressible Navier-Stokes equations. Our results are a continuation of the experiments with applying adaptivity to simulations of viscous incompressible flows made by Oden (1994), Ainsworth and Oden (1993), Oden et al. (1990), (1991), (1993), (1994). Their solutions were based on quadrilateral and brick elements with constrained approximation while we use triangular elements with the Rivara and irregular refinement techniques. The work is organized as follows. Section 2 states the flow problem. Section 3 presents the pressure correction method of Chorin (1973) to solve the Navier-Stokes equations. A residual error estimation technique due to Oden et al. (1994) and the adaptive strategy is discussed in Sections 4 and 5. The concluding part of the paper presents numerical examples.

2. The Navier-Stokes equations and the weak formulation

Incompressible flows of viscous fluids satisfy the Navier-Stokes equations. The state variables are selected as the velocity vector $\boldsymbol{u} = [u_1, u_2]$ and the pressure p. The Navier-Stokes equations express the balance of momentum and the conservation of mass (incompressibility)

$$\begin{aligned} &\boldsymbol{u}_{,t} + (\boldsymbol{u}\cdot\nabla)\boldsymbol{u} - \nabla\cdot 2\nu\varepsilon(u) + \nabla p = \boldsymbol{f} && \text{in} \quad \Omega \\ &\nabla\cdot\boldsymbol{u} = 0 && \text{in} \quad \Omega \\ &\boldsymbol{u} = \hat{\boldsymbol{u}} && \text{on} \quad \Gamma_D \\ &\boldsymbol{\sigma}(\boldsymbol{u}, p)\cdot\boldsymbol{n} = \boldsymbol{g} && \text{on} \quad \Gamma_N \end{aligned} \tag{2.1}$$

with the initial condition

$$\boldsymbol{u}(\boldsymbol{x}, 0) = \boldsymbol{u}_0(\boldsymbol{x}) \qquad \nabla\cdot\boldsymbol{u}_0 = 0 \tag{2.2}$$

In the above ν denotes the kinematic viscosity of the fluid, $\boldsymbol{\varepsilon}(\boldsymbol{u}) = 1/2(\nabla \boldsymbol{u} + \nabla \boldsymbol{u}^{\top})$ is the deformation rate tensor, $\boldsymbol{\sigma}(\boldsymbol{u}, p) = 2\nu\boldsymbol{\varepsilon}(\boldsymbol{u}) - \mathbf{I}p$ stands for the stress tensor. Γ_D and Γ_N are the parts of the boundary $\partial\Omega$ of the computational domain Ω, on which the Dirichlet and Neumann boundary conditions were specified, $\hat{\boldsymbol{u}}$ and $\boldsymbol{g}$ are the velocity and the stress defined on Γ_D and Γ_N, respectively. $\boldsymbol{f}$ is the field of body forces.

Multiplying Eqs $(2.1)_1$ and $(2.1)_2$ by the test functions $\boldsymbol{v}$ and q and integrating over the computational domain Ω we obtain a weak formulation of the Navier-Stokes equations:

find $\boldsymbol{u}(\boldsymbol{x}, t)$, $p(\boldsymbol{x}, t)$ such that

$$\begin{aligned} &\int_{\Omega} \boldsymbol{u}_{,t} \cdot \boldsymbol{v}\, dx + \int_{\Omega} (\boldsymbol{u} \cdot \nabla)\boldsymbol{u} \cdot \boldsymbol{v}\, dx + \int_{\Omega} 2\nu\boldsymbol{\varepsilon}(\boldsymbol{u}) : \boldsymbol{\varepsilon}(\boldsymbol{u})\, dx - \int_{\Omega} p\nabla \cdot \boldsymbol{v}\, dx = \\ &= \int_{\Omega} \boldsymbol{f} \cdot \boldsymbol{v}\, dx + \int_{\Gamma_N} \boldsymbol{g} \cdot \boldsymbol{v}\, dS \\ &\int_{\Omega} \nabla \cdot \boldsymbol{u} q\, dx = 0 \end{aligned} \tag{2.3}$$

The spaces of trial functions for velocities $\boldsymbol{u}$ and pressure p are defined as follows:

— the space of velocities

$$V = \left\{ \boldsymbol{v} \in \left(H^1(\Omega) \right)^2 : \ \boldsymbol{v} = \boldsymbol{0} \right. \tag{2.4}$$

— the space of pressures

$$M = \left\{ q \in L^2(\Omega);\ \text{if } \Gamma_D = \partial\Omega,\ \text{than additionally } \int_{\Omega} q\, dx = 0 \right\} \tag{2.5}$$

With these definitions we seek for a solution $\boldsymbol{u} \in \hat{\boldsymbol{u}} + L^2(0, T; V)$, $p \in L^2(0, T; M)$, where $[0, T]$ denotes the time interval.

The weak formulation (2.3) is equivalent to the formulation (2.1) of the flow problem (called "strong" in this context) providing the solution $\boldsymbol{u}$, p and the test functions $\boldsymbol{v}$, q are sufficiently smooth. (Derivation of Eqs (2.3) from Eq (2.1) was given above, the opposite implication can be shown by selecting the test functions $\boldsymbol{v}$ such that $\boldsymbol{v} = 0$ on Γ_D and integrating eq $(2.3)_1$ by parts.) The weak formulation can be considered, however, in a wider class of functions from the Sobolev spaces. It can be interpreted analogously as the principle of virtual works in linear elasticity.

For the stationary Navier-Stokes equations ($u_{,t} \equiv 0$) and with $\Gamma_D \equiv \partial\Omega$, the existance and uniqueness of the solution of Eq (2.3) can be shown (cf Girault and Raviart (1986)).

3. Pressure correction methods (projection methods) of A. Chorin

The weak formulation (2.3) is a basis for introducing the finite element discretization of the Navier-Stokes equations. Unlike in the case of classical elliptic boundary value problems the incompressibility condition $(2.3)_2$ restricts severely the class of element spaces that can be applied as well as the time discretization scheme of the problem. Automatic satisfaction of the incompressibility was the inspiration of developing a number of "incompressible elements", which are useful in discretization of the Navier-Stokes equations (for an account of finite element methods for fluid mechanics see Becker (1985)). Yet, in general, these approaches seem to be rather cumbersome in the context of adaptive methods as they involve lowered order of approximation of the pressure or suffer other drawbacks.

A successful application of adaptivity to the finite element simulations of the Navier-Stokes equations was recently presented by Oden (1994), Ainsworth and Oden (1992), Oden et al. (1990), (1991), (1993), (1994). The algorithm employed for solving flow problems was a version of the pressure correction scheme due to Chorin (1968), (1973) (also referred to as the projection method, a review of methods of this class is given in a work of Gresho and Chan (1990)).

The features of the pressure correction methods which make them especially attractive in combination with adaptivity can be listed as follows:

- The formulations are independent of the finite element approximation, which suggests a possibility of using adaptive meshes
- The algorithm is a multi-step method. Each of the steps is a classical elliptic boundary value problem. This enables one to use many standard and efficient finite element algorithms as *a posteriori* error estimation or iterative equation solvers.

The basic idea of the projection methods can be explained as follows. We express the Navier-Stokes equations in the form of the special evolutionary problem

$$\begin{aligned} \boldsymbol{u}_{,t} + \nabla p &= S(\boldsymbol{u}) \\ \nabla \cdot \boldsymbol{u} &= 0 \end{aligned} \tag{3.1}$$

where

$$S(\boldsymbol{u}) \equiv 2\nu \nabla \cdot \varepsilon(\boldsymbol{u}) + \boldsymbol{f} - (\boldsymbol{u} \cdot \nabla)\boldsymbol{u} \tag{3.2}$$

Equation (3.1) can be interpreted as a continuous projection of the field $S(\boldsymbol{u})$ onto the space of solenoidal functions (i.e. $\boldsymbol{u}_{,t}$) and the space of irrotational functions (i.e. ∇p). This continuous process can be approximated in time by performing the two projections at discrete time instants $\Delta t, 2\Delta t, \ldots, k\Delta t$, thus leading to the algorithm:

1. Given an initial velocity field $\boldsymbol{u}$ such that $\nabla \cdot \boldsymbol{u} = 0$
2. Anticipate the field $\nabla \tilde{p}(\boldsymbol{x}, t)$, $t \in [0, \Delta t]$, being approximation of ∇p
3. Solve the evolutionary problem: $\tilde{\boldsymbol{u}}_{,t} + \nabla \tilde{p} = S(\tilde{\boldsymbol{u}})$, $t \in [0, \Delta t]$
4. Project $\tilde{\boldsymbol{u}}(\Delta t)$ onto the space of solenoidal functions. Call the result $\boldsymbol{u}(\Delta t)$
5. Go to 1.

There exists a few implementations of the scheme outlined above. They are obtained by different selections of the algorithm defining $\tilde{p}$, different time integration schemes used to integrate the evolutionary problem and appropriate ways to perform the projection of step 4. The use of specific procedures in these steps influences the time accuracy of the scheme, the accuracy of satisfying boundary conditions, the stability and the cost of calculations. From a number of algorithms presented in the review work (cf Gresho and Chan (1990)) we chose two schemes which are advocated by the authors especially useful. The methods are called "Projection 1" and "Projection 2". Below we list subsequent steps of the two methods. For the details of derivation of the schemes see Gresho and Chan (1990).

"Projection 1" method

Set $m = 0$.

1. Find $\boldsymbol{u}_{m+1/2}$ such that

$$\begin{aligned} &\frac{\boldsymbol{u}_{m+1/2}-\boldsymbol{u}_m}{\Delta t}=\frac{1}{2}\nabla\cdot[2\nu\varepsilon(\boldsymbol{u}_{m+1/2}+\boldsymbol{u}_m)]+\boldsymbol{F}_m && \text{in} \quad \Omega \\ &\boldsymbol{u}_{m+1/2}=\hat{\boldsymbol{u}}(t_{m+1}) && \text{on} \quad \Gamma_D \\ &2\nu\varepsilon(\boldsymbol{u}_{m+1/2})\boldsymbol{n}=\boldsymbol{g}+\boldsymbol{n}p_m && \text{on} \quad \Gamma_N \end{aligned} \tag{3.3}$$

where $\boldsymbol{F}_m := -(\boldsymbol{u}_m\cdot\nabla)\boldsymbol{u}_m+\boldsymbol{f}(t_m)$, $\boldsymbol{n}$ is the unit normal vector on $\partial\Omega$. The above is equivalent to solving the following elliptic problem

$$\boldsymbol{u}_{m+1/2}-\frac{\Delta t}{2}\nabla\cdot[2\nu\varepsilon(\boldsymbol{u}_{m+1/2})]=\boldsymbol{u}_m+\frac{\Delta t}{2}\nabla\cdot[2\nu\varepsilon(\boldsymbol{u}_m)]+\Delta t\boldsymbol{F}_m \tag{3.4}$$

2. Find ϕ such that

$$\begin{aligned} &-\nabla^2\phi=-\nabla\cdot\boldsymbol{u}_{m+1/2} && \text{in} \quad \Omega \\ &\frac{\partial\phi}{\partial n}=0 && \text{on} \quad \Gamma_D \\ &\phi=-\Delta t g_m\cdot\boldsymbol{n} && \text{on} \quad \Gamma_N \end{aligned} \tag{3.5}$$

3. Express $\boldsymbol{u}_{m+1}$ as

$$\begin{aligned} &\boldsymbol{u}_{m+1}=\boldsymbol{u}_{m+1/2}-\nabla\phi && \text{in} \quad \Omega \\ &\boldsymbol{u}_{m+1}=\hat{\boldsymbol{u}}_{m+1} && \text{on} \quad \Gamma_D \end{aligned} \tag{3.6}$$

4. Update the pressure

$$p_{m+1}=\frac{1}{\Delta t}\phi \tag{3.7}$$

The problems listed in steps 1,2 and 3 are equivalent to the following weak formulations:

1. Find $\boldsymbol{u}_{m+1/2}$ such that $\boldsymbol{u}_{m+1/2}=\hat{\boldsymbol{u}}_{m+1}$ on Γ_D and

$$\begin{aligned} &\int_\Omega \boldsymbol{u}_{m+1/2}\cdot\boldsymbol{v}\,dx+\frac{\Delta t}{2}\int_\Omega 2\nu\varepsilon(\boldsymbol{u}_{m+1/2}):\varepsilon(\boldsymbol{v})\,dx=\int_\Omega \boldsymbol{u}_m\cdot\boldsymbol{v}dx+ \\ &-\frac{\Delta t}{2}\int_\Omega 2\nu\varepsilon(\boldsymbol{u}_m):\varepsilon(\boldsymbol{v})\,dx+\Delta t\int_\Omega \boldsymbol{f}_m\cdot\boldsymbol{v}\,dx-\Delta t\int_\Omega(\boldsymbol{u}_m\cdot\boldsymbol{\nabla})\boldsymbol{u}_m\cdot\boldsymbol{v}\,dx+ \\ &+\frac{\Delta t}{2}\int_{\Gamma_N}(\boldsymbol{g}+\boldsymbol{n}p_m)\cdot\boldsymbol{v}\,dS+\frac{\Delta t}{2}\int_{\Gamma_N}2\nu[\varepsilon(\boldsymbol{u}_m)\boldsymbol{n}]\cdot\boldsymbol{v}\,dS \quad \forall\boldsymbol{v}=0 \text{ on } \Gamma_D \end{aligned} \tag{3.8}$$

2. Find ϕ such that $\phi=-\Delta t g_n\cdot\boldsymbol{n}$ on Γ_N and

$$\int_\Omega \nabla\phi\cdot\nabla q\,dx=-\int_\Omega \nabla\cdot\boldsymbol{u}_{m+1/2}q\,dx \qquad \forall q=0 \text{ on } \Gamma_N \tag{3.9}$$

3. Find $\boldsymbol{u}_{m+1}$ such that $\boldsymbol{u}_{m+1} = \widehat{\boldsymbol{u}}_{m+1}$ on Γ_D and

$$\int_\Omega \boldsymbol{u}_{m+1} \cdot \boldsymbol{v} dx = \int_\Omega \boldsymbol{u}_{m+1/2} \cdot \boldsymbol{v} dx - \int_\Omega \nabla\phi \cdot \boldsymbol{v}\, dx \qquad \forall \boldsymbol{v} = 0 \text{ on } \Gamma_D \quad (3.10)$$

In step 3 we apply the L^2-projection to make $\boldsymbol{u}_{m+1}$ a member of the finite element space.

"Projection 2" method

1. Given field $\boldsymbol{u}_0$ such that $\nabla \cdot \boldsymbol{u}_0 = 0$ find the pressure p_0

$$\begin{aligned} -\nabla^2 p_0 &= \nabla^2 \boldsymbol{F}(\boldsymbol{u}_0) && \text{in} \quad \Omega \\ \frac{\partial p_0}{\partial n} &= \boldsymbol{n} \cdot \left[2\nu\nabla \cdot \varepsilon(\boldsymbol{u}_0) + \boldsymbol{F}(\boldsymbol{u}_0) - \frac{d}{dt}\widehat{\boldsymbol{u}}_0\right] && \text{on} \quad \Gamma_D \\ p_0 &= \nu \frac{\partial(\boldsymbol{u}_0 \cdot \boldsymbol{n})}{\partial n} - \boldsymbol{F}(\boldsymbol{u}_0) \cdot \boldsymbol{n} && \text{on} \quad \Gamma_N \end{aligned} \quad (3.11)$$

where $\boldsymbol{F}(\boldsymbol{u}) = \boldsymbol{f} - (\boldsymbol{u} \cdot \nabla)\boldsymbol{u}$.

Set $m = 0$.

2. Find $\boldsymbol{u}_{m+1/2}$ such that

$$\begin{aligned} &\frac{\boldsymbol{u}_{m+1/2} - \boldsymbol{u}_m}{\Delta t} + \nabla p_m = \tfrac{1}{2}\nabla \cdot [2\nu\varepsilon(\boldsymbol{u}_{m+1/2} + \boldsymbol{u}_m)] + \boldsymbol{F}(\boldsymbol{u}_m) && \text{in} \quad \Omega \\ &\boldsymbol{u}_{m+1/2} = \widehat{\boldsymbol{u}}_{m+1} && \text{on} \quad \Gamma_D \\ &2\nu\varepsilon(\boldsymbol{u}_{m+1/2})\boldsymbol{n} = \boldsymbol{g} + \boldsymbol{n}p_m && \text{on} \quad \Gamma_N \end{aligned} \quad (3.12)$$

The above is equivalent to solving the following elliptic boundary value problem

$$\boldsymbol{u}_{m+1/2} - \frac{\Delta t}{2}\nabla \cdot [2\nu\varepsilon(\boldsymbol{u}_{m+1/2})] = \boldsymbol{u}_m + \frac{\Delta t}{2}\nabla \cdot [2\nu\varepsilon(\boldsymbol{u}_m)] + \Delta t(\boldsymbol{F}_m - \nabla p_m) \quad (3.13)$$

3. Find ϕ such that

$$\begin{aligned} -\nabla^2\phi &= -\nabla \cdot \boldsymbol{u}_{m+1/2} && \text{in} \quad \Omega \\ \frac{\partial\phi}{\partial n} &= 0 && \text{on} \quad \Gamma_D \\ \phi &= -\frac{\Delta t}{2}(\boldsymbol{F}_{m+1} \cdot \boldsymbol{n} + p_m) && \text{on} \quad \Gamma_N \end{aligned} \quad (3.14)$$

4. Update the velocities

$$\begin{aligned} \boldsymbol{u}_{m+1} &= \boldsymbol{u}_{m+1/2} - \nabla\phi && \text{in} \quad \Omega \\ \boldsymbol{u}_{m+1} &= \widehat{\boldsymbol{u}}_{m+1} && \text{on} \quad \Gamma_D \end{aligned} \quad (3.15)$$

5. Update the pressure

$$p_{m+1} = p_m + \frac{2}{\Delta t}\phi \tag{3.16}$$

6. Go to 2.

The problems listed in steps 1,2,3 and 4 are equivalent to solving the following weak formulations:

1. Find p_0 such that $p_0 = \nu\partial(\boldsymbol{u}_0 \cdot \boldsymbol{n})/\partial n - \boldsymbol{F}(\boldsymbol{u}_0) \cdot \boldsymbol{n}$ on Γ_N and

$$\int_\Omega \nabla p_0 \cdot \nabla q \, dx = \int_\Omega \boldsymbol{F}(u_0) \cdot \nabla q \, dx - \int_{\Gamma_D} \boldsymbol{F} \cdot \boldsymbol{n} q \, dS \qquad \forall q = 0 \text{ on } \Gamma_N \tag{3.17}$$

2. Find $\boldsymbol{u}_{m+1/2}$ such that $\boldsymbol{u}_{m+1/2} = \hat{\boldsymbol{u}}_{m+1}$ on Γ_D and

$$\begin{aligned} &\int_\Omega \boldsymbol{u}_{m+1/2} \cdot \boldsymbol{v} \, dx + \frac{\Delta t}{2} \int_\Omega 2\nu\varepsilon(\boldsymbol{u}_{m+1/2}) : \varepsilon(\boldsymbol{v}) \, dx = \int_\Omega \boldsymbol{u}_m \cdot \boldsymbol{v} dx + \\ &-\frac{\Delta t}{2} \int_\Omega 2\nu\varepsilon(\boldsymbol{u}_m) : \varepsilon(\boldsymbol{v}) \, dx - \Delta t \int_\Omega (\boldsymbol{u}_m \cdot \nabla)\boldsymbol{u}_m \cdot \boldsymbol{v} \, dx - \Delta t \int_\Omega \nabla p_m \cdot \boldsymbol{v} \, dx + \\ &+\frac{\Delta t}{2} \int_{\Gamma_N} (\boldsymbol{g}_{m+1} + \boldsymbol{n} p_m) \cdot \boldsymbol{v} \, dS + \frac{\Delta t}{2} \int_{\Gamma_N} 2\nu[\varepsilon(\boldsymbol{u}_m)\boldsymbol{n}] \cdot \boldsymbol{v} \, dS + \\ &+\int_\Omega \boldsymbol{f} \cdot \boldsymbol{v} \, dx \qquad \forall \boldsymbol{v} = 0 \text{ on } \Gamma_D \end{aligned} \tag{3.18}$$

3. Find ϕ such that $\phi = -\Delta t/2[\boldsymbol{F}_{m+1} \cdot \boldsymbol{n} + p_m]$ on Γ_N and

$$\int_\Omega \nabla\phi \cdot \nabla q \, dx = -\int_\Omega \nabla \cdot \boldsymbol{u}_{m+1/2} q \, dx \qquad \forall q = 0 \text{ on } \Gamma_N \tag{3.19}$$

4. Find $\boldsymbol{u}_{m+1}$ such that: $\boldsymbol{u}_{m+1} = \hat{\boldsymbol{u}}_{m+1}$ on Γ_D and

$$\int_\Omega \boldsymbol{u}_{m+1} \cdot \boldsymbol{v} \, dx = \int_\Omega \boldsymbol{u}_{m+1/2} \cdot \boldsymbol{v} \, dx - \int_\Omega \nabla\phi \cdot \boldsymbol{v} \, dx \qquad \forall \boldsymbol{v} = 0 \text{ on } \Gamma_D \tag{3.20}$$

The use of the L^2-projection in step 4 is motivated as in the previous method.

The following features of the projection methods should be emphasized:

1. The procedures consist of three steps

2. The weak formulations corresponding to the subsequent steps are symmetric and positive definite

3. If the time step Δt is fixed, the stiffness matrices corresponding to boundary-value problems do not change in time. This allows one to compute and decompose them in the first step and then to use the resolution feature of the equation solver.

"Projection 2" is $O(\Delta t^3)$ accurate in time while "Projection 1" is only $O(\Delta t^2)$. An advantage of "Projection 2" is that the stationary solution satisfies the weak formulation of the Navier-Stokes equations which for "Projection 1" is satisfied only approximately. On the other hand "Projection 1" is considered more stable.

4. An a posteriori error estimate for finite approximations of the Navier-Stokes equations

A successful application of adaptive methods requires a reliable *a posteriori* error estimation technique, i.e. a procedure estimating errors of an existing finite element approximation of the problem. Element error indicators are used to indicate regions with big errors where enrichment of the mesh (refinement) is necessary.

A number of error estimation techniques have been developed for linear elliptic boundary-value problems. A list of them includes interpolation errors, estimates based on post-processing, techniques using duality and residual error estimates. Estimation of errors of more complex, nonlinear and other than elliptic problems is most often done by using estimates valid for linear elliptic equations to linear steps of iterative solving of a given problem. One exception to this rule is the residual error estimate due to Oden et al. (1994), which is proven to estimate the error of the original Navier-Stokes equations. This section outlines basic components and implementation details of the method.

4.1. A general idea of the estimate

4.1.1. Definition of the norm

Let $\boldsymbol{e} := \boldsymbol{u} - \boldsymbol{u}_h$ and $E = p - p_h$ denote the errors in the velocity and in the pressure of the finite approximations $\boldsymbol{u}_h$ and p_h. We assume that $\boldsymbol{u}_h$ and

p_h satisfy the weak formulation of the Navier-Stokes equations, i.e. Eq (2.3) with $\boldsymbol{u}_{h,t} = 0$. We define the auxiliary functions $\boldsymbol{\phi} \in V$ and $\psi \in M$ which solve the following boundary value problem

$$\begin{aligned}\int_\Omega 2\nu\varepsilon(\boldsymbol{\phi}) : \varepsilon(\boldsymbol{v})\, dx &= \int_\Omega 2\nu\varepsilon(\boldsymbol{e}) : \varepsilon(\boldsymbol{v})\, dx - \int_\Omega E\nabla\cdot\boldsymbol{v}\, dx + \\ &+ \int_\Omega (\boldsymbol{u}\cdot\nabla)\boldsymbol{u}\cdot\boldsymbol{v}\, dx - \int_\Omega (\boldsymbol{u}_h\cdot\nabla)\boldsymbol{u}_h\cdot\boldsymbol{v}\, dx \qquad \forall \boldsymbol{v} \in V \\ \int_\Omega \psi q\, dx &= -\int_\Omega \nabla\cdot\boldsymbol{e} q\, dx \qquad \forall q \in M\end{aligned} \tag{4.1}$$

The norm of a pair $(\boldsymbol{e}, E)$ is defined as follows

$$\|(\boldsymbol{e}, E)\|_*^2 = \int_\Omega 2\nu\varepsilon(\boldsymbol{\phi},\boldsymbol{\phi})\, dx + \int_\Omega \psi^2\, dx \tag{4.2}$$

This norm turns out to be equivalent to the standard combination of the H^1 and L^2 norms, $|\cdot|_1$ and $\|\cdot\|_0$, used for the Navier-Stokes equations: there exist constants $k_1 > 0$, $k_2 > 0$ such that, if the element size $h \to 0$ then

$$k_1\|(\boldsymbol{e}, E)\|_*^2 \le (1 + O(h))|\boldsymbol{e}|_1^2 + \|E\|_0^2 \le k_2\|(\boldsymbol{e}, E)\|_*^2 \tag{4.3}$$

4.1.2. Evaluation of error indicators

Let $\boldsymbol{\phi}_K$ and ψ_K ("error indicator functions") be defined on elements K as solutions of the following local problems

$$\int_K 2\nu\varepsilon(\boldsymbol{\phi}_K) : \varepsilon(\boldsymbol{v})\, dx = \int_{\partial K\cap\Gamma_N} \boldsymbol{g}\cdot\boldsymbol{v} dS + \int_K \boldsymbol{f}\cdot\boldsymbol{v}\, dx - \int_K 2\nu\varepsilon(\boldsymbol{u}_h) : \varepsilon(\boldsymbol{v})\, dx + \tag{4.4}$$

$$+ \int_K p_h\nabla\cdot\boldsymbol{v}\, dx - \int_K (\boldsymbol{u}_h\cdot\nabla)\boldsymbol{u}_h\cdot\boldsymbol{v}\, dx + \int_{\partial K} \langle \boldsymbol{n}_K\cdot\boldsymbol{\sigma}(\boldsymbol{u}_h, p_h)\rangle_{1-\alpha}\cdot\boldsymbol{v}\, dS \qquad \forall \boldsymbol{v} \in V|_K$$

$$\int_K \psi_K q\, dx = \int_K \nabla\cdot\boldsymbol{u}_h q\, dx \qquad \forall q \in M|_K \tag{4.5}$$

Then

$$\|(\boldsymbol{e}, E)\|_*^2 \le \sum_K \eta_K^2 \tag{4.6}$$

where

$$\eta_K^2 = \int_K 2\nu\varepsilon(\boldsymbol{\phi}_k) : \varepsilon(\boldsymbol{\phi}_k)\, dx + \int_K (\nabla\cdot\boldsymbol{u}_h)^2\, dx \tag{4.7}$$

In Eq (4.4) $\langle \boldsymbol{n}_K \cdot \boldsymbol{\sigma}(\boldsymbol{u}_h, p_h)\rangle_{1-\alpha}$ denotes the stress along the interelement boundary evaluated as a special average of the stress in a given element and in the adjacent element. This avaraged stress must be in equilibrium with the remaining forces loading the element which is the key point of the method.

4.2. Evaluation of self-equilibrated stresses

The weak formulation (4.4) corresponds to the Neumann problem of linear elasticity. It is solvable only if the forces on the right-hand side of (4.4) are in equilibrium. Such an equilibrium can be attained by appropriate averaging of stresses along interelement boundaries. An efficient procedure for evaluation of self-equilibrated stresses (fluxes) was developed by Ainsworth and Oden (1992). Its application to the Navier-Stokes equations can be outlined as follows.

- Consider the "Projection 2" method. Adding the weak statements (3.18) and (3.20) results in

$$
\begin{aligned}
0 = &\int_{\Gamma_N} \Big\{\frac{1}{2}[(\boldsymbol{g} + \boldsymbol{n}p_m) + 2\nu\varepsilon(\boldsymbol{u}_m)\boldsymbol{n}] - \boldsymbol{n}p_m\Big\} \cdot \boldsymbol{v}\, dS + \int_{\Omega} \boldsymbol{f} \cdot \boldsymbol{v}\, dx + \\
&- \int_{\Omega} (\boldsymbol{u}_m \cdot \nabla)\boldsymbol{u}_m \cdot \boldsymbol{v}\, dx - 2\nu \int_{\Omega} \frac{1}{2}[\varepsilon(\boldsymbol{u}_m) + \varepsilon(\boldsymbol{u}_{m+1/2})] : \varepsilon(\boldsymbol{v})\, dx + \\
&\int_{\Omega} \frac{1}{2}(p_m + p_{m+1})\nabla \cdot \boldsymbol{v}\, dx + \frac{1}{\Delta t}\int_{\Omega} (\boldsymbol{u}_m - \boldsymbol{u}_{m+1/2}) \cdot \boldsymbol{v}\, dx
\end{aligned}
\tag{4.8}
$$

We observe that if steady state is achieved, $\boldsymbol{u}_m = \boldsymbol{u}_{m+1} = \boldsymbol{u}_{m+1/2}$, $p_m = p_{m+1}$, the solution satisfies the weak formulation of the Navier-Stokes equations (except for the boundary term)

$$
\begin{aligned}
0 = &\int_{\Gamma_N} \Big\{\frac{1}{2}[(\boldsymbol{g} + \boldsymbol{n}p_h) + 2\nu\varepsilon(\boldsymbol{u}_h)\boldsymbol{n}] - \boldsymbol{n}p_h\Big\} \cdot \boldsymbol{v}\, dS + \int_{\Omega} \boldsymbol{f} \cdot \boldsymbol{v}\, dx + \\
&- \int_{\Omega} (\boldsymbol{u}_h \cdot \nabla)\boldsymbol{u}_h \cdot \boldsymbol{v}\, dx - 2\nu \int_{\Omega} \varepsilon(\boldsymbol{u}_h) : \varepsilon(\boldsymbol{v})\, dx + \int_{\Omega} p_h \nabla \cdot \boldsymbol{v}\, dx
\end{aligned}
\tag{4.9}
$$

where $\boldsymbol{u}_h, p_h$ is the steady state solution. Therefore, the residue of the first of the Navier-Stokes equations is a sum of the residues of the first and the third steps of the method.

- In Eq (4.4) the linear functional on the right-hand side corresponds to the residue of the stationary Navier-Stokes equations augmented by the virtual work of the averaged stress. This stress between elements K and L is defined using weighting functions $\alpha_{KL}^{(k)}$ and $\alpha_{LK}^{(k)}$, $k = 1,2$ defined along the common boundary Γ_{KL}, $\alpha_{KL}^{(k)}(s) + \alpha_{LK}^{(k)}(s) \equiv 1$

$$\langle \boldsymbol{n}_K \cdot \boldsymbol{\sigma}(\boldsymbol{u}_h, p_h)\rangle^{(k)} = \boldsymbol{n}_K \cdot \left[\alpha_{LK}^{(k)} \boldsymbol{\sigma}_K^{(k)}(\boldsymbol{u}_h, p_h) + \alpha_{KL}^{(k)} \boldsymbol{\sigma}_L^{(k)}(\boldsymbol{u}_h, p_h)\right] \tag{4.10}$$

where $\boldsymbol{\sigma}_K^{(k)}$, $\boldsymbol{\sigma}_L^{(k)}$ are the kth components of the stress in element K or L, respectively. It is sufficient to assume that $\alpha_{KL}^{(k)}$ is a linear function to make the self-equilibration possible.

- The procedure of establishing $\alpha_{KL}^{(k)}(s)$ for the element K can be outlined as follows:

1. We identify the actual vertex nodes $\mathcal{A}$ of element K. In the case of 1-irregular meshes (with constraints) these vertices do not necessarily coincide with the ordinary nodes of K: actual nodes correspond to the global degrees of freedom which define the solution in the element, they are sometimes located outside of the element. With every node A and with every element-neighbor L of K we associate parameters $\alpha_{KL,A}^{(k)}$ and $\alpha_{LK,A}^{(k)}$. The functions $\alpha_{KL}^{(k)}(s)$ shall be expressed as follows

$$\alpha_{KL}^{(k)}(s) = \sum_{A \in \mathcal{A}} \alpha_{KL,A}^{(k)} \psi_A(s) \tag{4.11}$$

where ψ_A are the global linear base shape functions associated with nodes A.

2. For every actual node A of element K we identify all the remaining elements L for which A is a node, too – a patch of elements.

3. For every element L, and for every pair K, L of elements in the patch we evaluate the quantities

$$\begin{aligned} b_{L,A}^{(k)} = & \int_{\partial L \cap \Gamma_N} \boldsymbol{g} \cdot \boldsymbol{\psi}_A^{(k)}\, dS + \int_L \boldsymbol{f} \cdot \boldsymbol{\psi}_A^{(k)}\, dx + \\ & - \int_L (\boldsymbol{u}_h \cdot \nabla)\boldsymbol{u}_h \cdot \boldsymbol{\psi}_A^{(k)}\, dx - 2\nu \int_K \varepsilon(\boldsymbol{u}_h) : \varepsilon(\boldsymbol{\psi}_A^{(k)})\, dx + \\ & + \int_K p_h \nabla \cdot \boldsymbol{\psi}_A^{(k)}\, dx + \int_{\partial K \setminus \partial\Omega} \langle \boldsymbol{n}_K \cdot \boldsymbol{\sigma}(\boldsymbol{u}_h, p_h)\rangle_{1/2} \cdot \boldsymbol{\psi}_A^{(k)}\, dS \qquad k = 1,2 \end{aligned} \tag{4.12}$$

$$\varrho_{KL,A}^{(k)} = \int_{\Gamma_{KL}} [\boldsymbol{n}_K \cdot \boldsymbol{\sigma}_K(\boldsymbol{u}_h, p_h) + \boldsymbol{n}_L \cdot \boldsymbol{\sigma}_L(\boldsymbol{u}_h, p_h)] \cdot \boldsymbol{\psi}_A^{(k)}\, dS \qquad k = 1,2 \tag{4.13}$$

where $\boldsymbol{\psi}_A^{(1)} = (\psi_A, 0)$, $\boldsymbol{\psi}_A^{(2)} = (0, \psi_A)$ are the global vector base shape functions associated with A. Parameters $b_{K,A}^{(k)}$ correspond to the residue on K evaluated with stresses averaged with weights 1/2. $\varrho_{KL,A}^{(k)}$ are expressed by a jump of stresses along Γ_{KL}.

4. For every patch of elements identified by nodes $\mathcal{A}$ we construct and solve the system of equations

$$\boldsymbol{T}_A \boldsymbol{\lambda}_A^{(k)} = \boldsymbol{b}_A^{(k)} \qquad k = 1, 2 \tag{4.14}$$

where $\boldsymbol{b}_A^{(k)} = \{b_{L,A}^{(k)}\}$, L – elements of the patch

$$\{\boldsymbol{T}_A\}_{LM} = \begin{cases} C_L & \text{if } L = M \\ -1 & \text{if elements } L \text{ and } M \text{ have a common edge} \\ 0 & \text{otherwise} \end{cases} \tag{4.15}$$

C_L denotes here the number of elements in the patch which share a common edge with the element L.

5. Set parameters $\alpha_{KL,A}^{(k)}$

$$\alpha_{KL,A}^{(k)} = \frac{1}{2} + \frac{\lambda_{K,A}^{(k)} - \lambda_{L,A}^{(k)}}{\varrho_{KL,A}^{(k)}} \tag{4.16}$$

6. Evaluate $\alpha_{KL}^{(k)}(s)$ according to Eq (4.11).

4.2.1. Details of numerical implementation

- As mentioned above the residue $b_{L,A}^{(k)}$ can be evaluated as a sum of the residues of step 1. and 3. of the "Projection 2" method. For "Projection 1" the situation is similar except for the fact that $\boldsymbol{u}_{m+1/2} \neq \boldsymbol{u}_m$.
- Averaging of the pressure as a component of $\boldsymbol{\sigma} = 2\nu\boldsymbol{\varepsilon}(\boldsymbol{u}_h) - \boldsymbol{I}p_h$ does not affect the equilibrium as p_h is continuous. Thus averaging is applied to viscous stresses only.
- Exact solutions of Eq (4.4) are, in general, unavailable. In practice they are approximated with finite element shape functions of the order extended from p to $p+1$ where p is the order of the original shape functions..
- If the jump of interelement stresses $\varrho_{KL,A}^{(k)}$ is very small then Eq (4.16) results in large round-off errors. In such situations, however, no averaging is necessary as the quantities being averaged are almost identical. In practice we set $\alpha_{KL,A}^{(k)} = 0.5$.

5. h-adaptive strategies

The idea of h-adaptivity consists in reducing of element sizes h in regions with large errors. The following mesh refinement techniques are in common use: Rivara method (cf Rivara (1984)), method of 1-irregular meshes (cf Demkowicz and Oden (1989)), "green" elements of Bank (cf Bank et al. 1983)) and remeshing (i.e. regenerating a mesh). In this work the first two methods are used.

The Rivara technique

In this approach elements are subdivided into two parts such that the longest side of an element is divided. At the same time an element-neighbor sharing the broken side is subsected. If this side is not its longest side, an attempt to divide the element-neighbor along its longest side is made, together with the subsequent neighbor, etc., until the subsection of two neighbors along their common longest side is obtained. An advantage of the method is that it does not introduce irregular nodes, i.e. the nodes which are vertices of one element and are located inside an edge of a neighboring element.

The method of 1-irregular meshes (constrained approximation)

The algorithm consists in breaking elements into 4 congruent "elements-sons". In this process irregular nodes mentioned above are generated. The presence of such nodes requires constraining degrees of freedom of neighboring elements to ensure the continuity of approximation, which can be considered a drawback of the method. The advantages include: a possibility of easy unrefinements (essential in transient problems) and a possibility of using some efficient iterative solvers (cf Rachowicz (1995)).

The algorithm of mesh adaptation

We follow a commonly accepted strategy of mesh adaptation consisting in subdividing elements with biggest errors. Its implementation to the Navier-Stokes flow solver is as follows:

1. Integrate the problem in time until the steady state is reached.

2. For all elements K evaluate error indicators η_K (4.7). Find $\eta_{max} = \max_K \eta_K$. Interrupt solving if $\eta_{max} \leq TOL$ with TOL being the prescribed tolerance.

3. Subsect elements K for which $\eta_K \geq \alpha \eta_{max}$, $0 < \alpha < 1$ is a fixed parameter.

4. Go to 1.

6. Numerical examples

The projection methods have been used to solve example problems of incompressible flows. They include flows in model computational domains of simple geometry as well as flows around airfoils. In these examples the Dirichlet boundary conditions were applied along the boundary of an obstacle as well as on the inflow of the computational domain and along its sides parallel to the flow. On the outflow boundary the Neumann boundary condition was applied with zero stress. The problems were integrated in time with the time step Δt correspoding to the Courant-Friedrichs-Levy number, $CFL = 0.5$ ($\Delta t = CFL \min_K(h_K/|\boldsymbol{u}|)$). Error indicators were calculated using the Wu-Oden-Ainsworth method and the adaptive strategy of the previous section was used to refine meshes.

Example 1: Cavity flow

A popular test problem, a cavity flow with the Reynolds number $\mathrm{Re} = 50$, was solved with the "Projection 2" method on a mesh of elements of the order $p = 2$. Fig.1a presents the geometry of the problem and an h-adaptive mesh with 3 levels of refinements. The method of 1-irregular meshes was used to generate adaptive meshes. Fig.1b-d present the steady state solution. It is characterized with singularities at upper corners of the computational domain and with a boundary layer along the upper edge.

Example 2: Flow in a backstep channel

The geometry of this problem and an h-adaptive mesh (order $p = 2$) are shown in Fig.2a. The problem was solved with the Reynolds number $\mathrm{Re} = 25$ (with respect to the diameter of the inflow). A parabolic profile of the velocity was assumed on the inflow boundary. Like in the previous example the 1-irregular mesh with 3 levels of refinements was generated. The solution obtained with the "Projection 2" method is presented in Fig.2b-d. It is significantly irregular around the step where we observe a singularity of the pressure and a recirculation zone. At some distance from the step the flow is practically uniform.

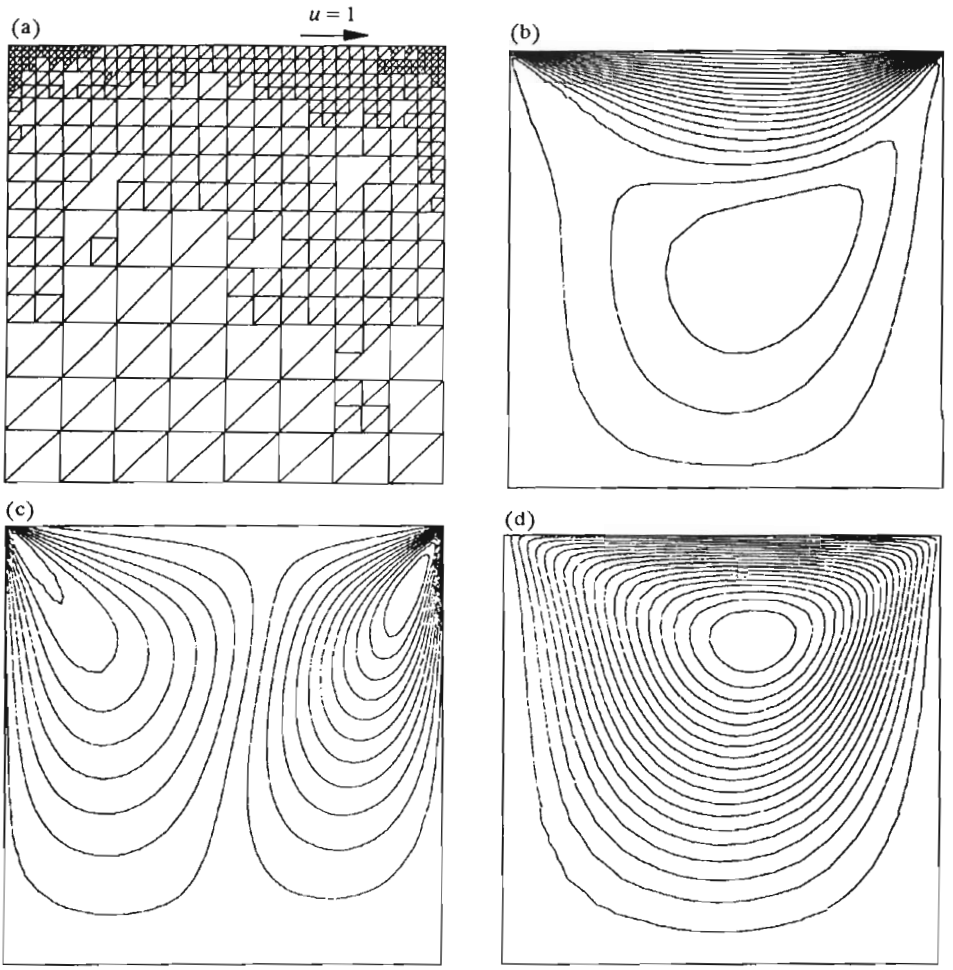

Fig. 1. Cavity flow, Re = 50, (a) statement of the problem and an h-adaptive mesh, (b) u_1 velocity component, (c) u_2 velocity component, (d) stream function

Example 3: Flow around a NACA 0012 airfoil

Flows around airfoils are typical problems of aerospace engineering. As a first of problems of this class we present an analysis of the flow around NACA 0012 airfoil with the angle of attack 5° and with the Reynolds number Re = 100. A rectangular computational domain around the airfoil was covered with an unstructured mesh of 900 linear elements distributed with nonuniform density allowing for an accurate approximation of the geometry. Fig.3a presents an h-adaptive mesh of 2100 elements obtained with 3 levels of

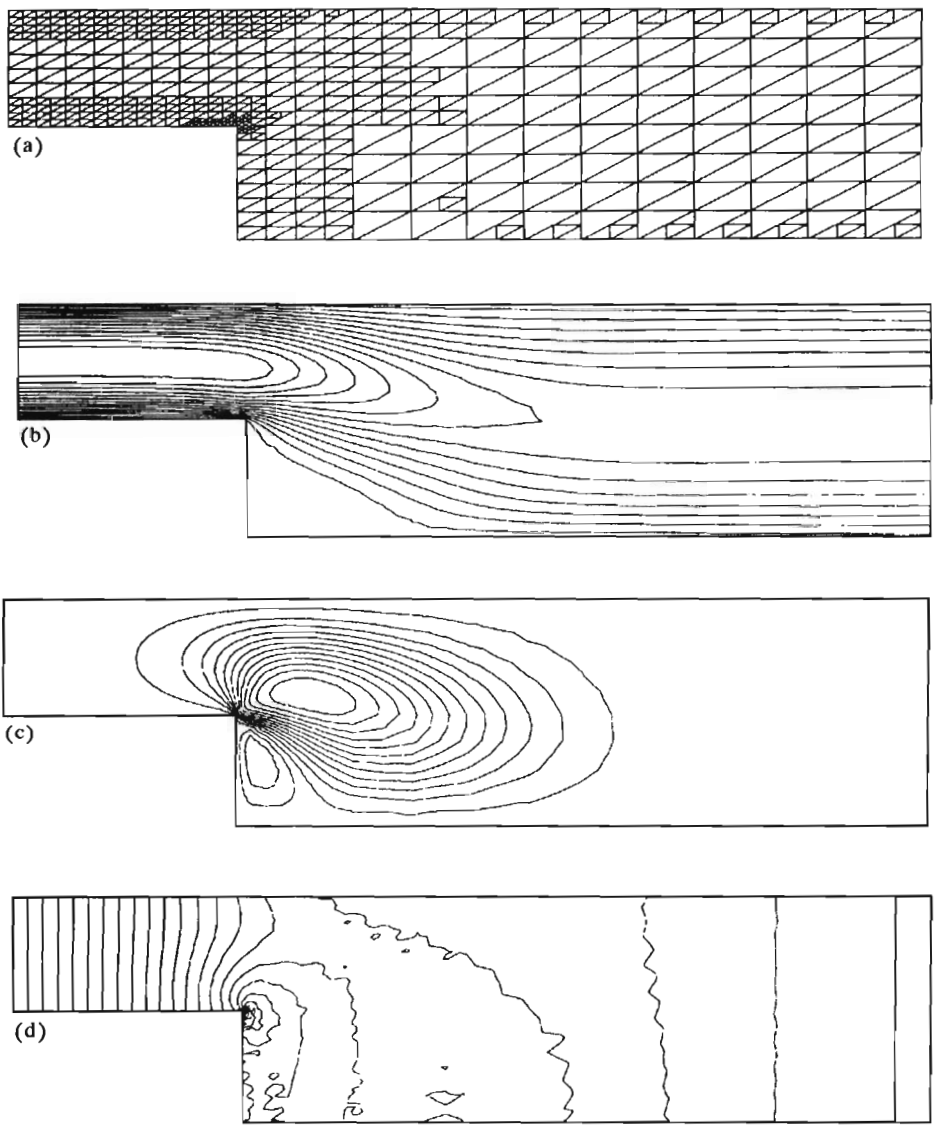

Fig. 2. Backstep channel problem, Re = 25, (a) geometry and an h-adaptive mesh, (b) u_1 velocity component, (c) u_2 velocity component, (d) distribution of pressure

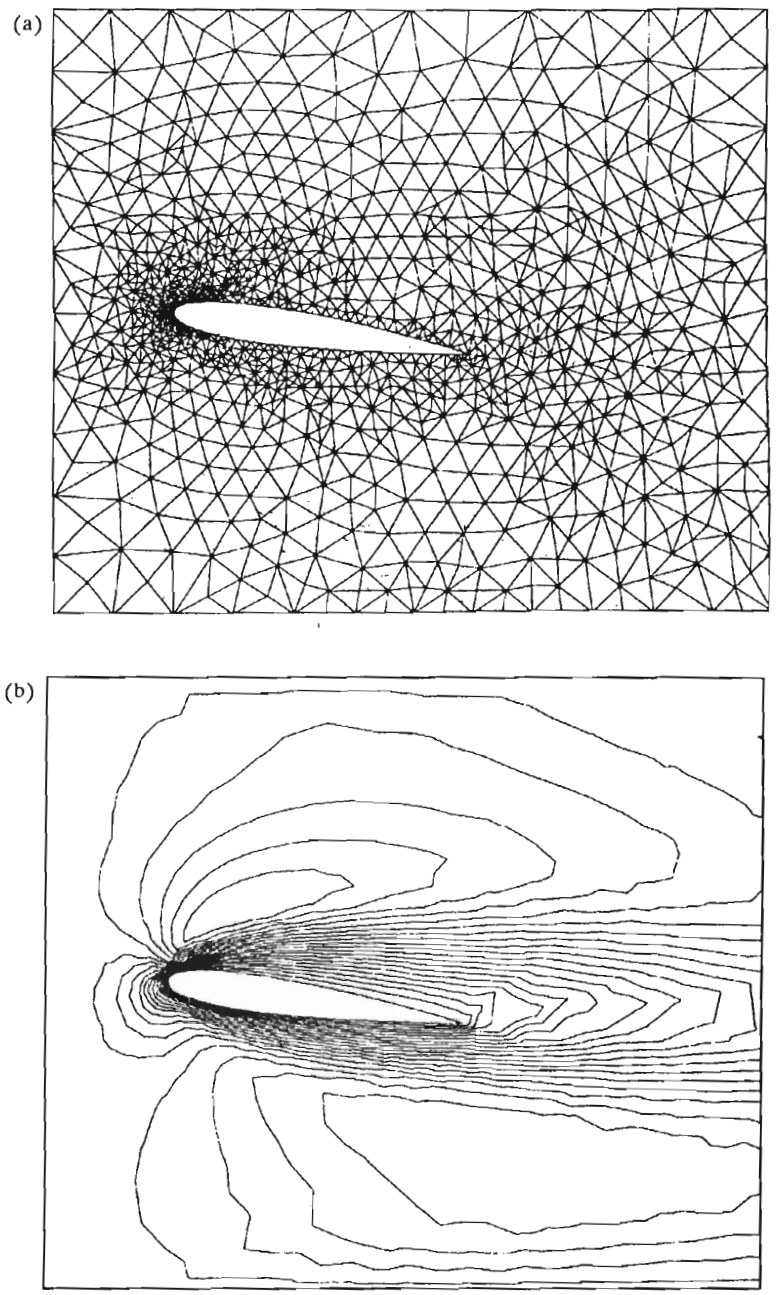

Fig. 3. Flow around NACA 0012 airfoil, Re = 100, (a) geometry and an h-adaptive mesh, (b) u_1 velocity component

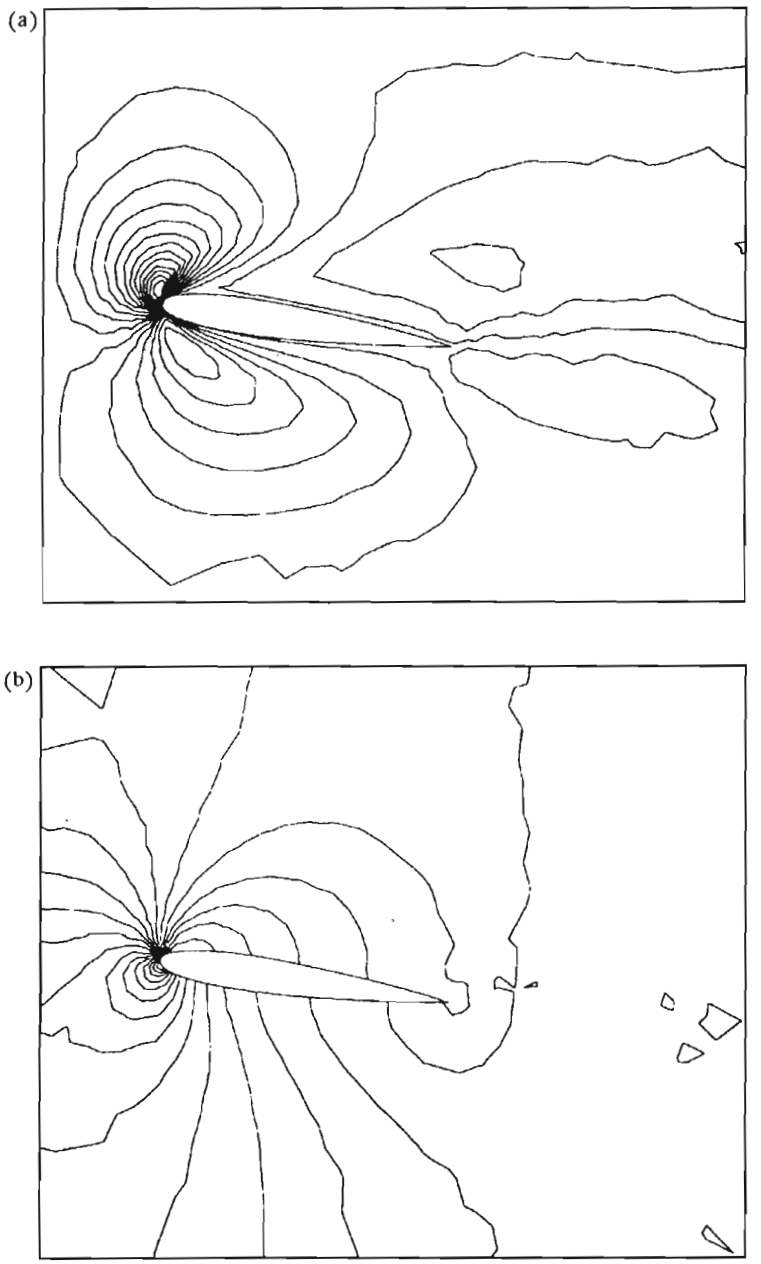

Fig. 4. Flow around NACA 0012 airfoil, Re = 100, (a) u_2 velocity component, (b) distribution of pressure

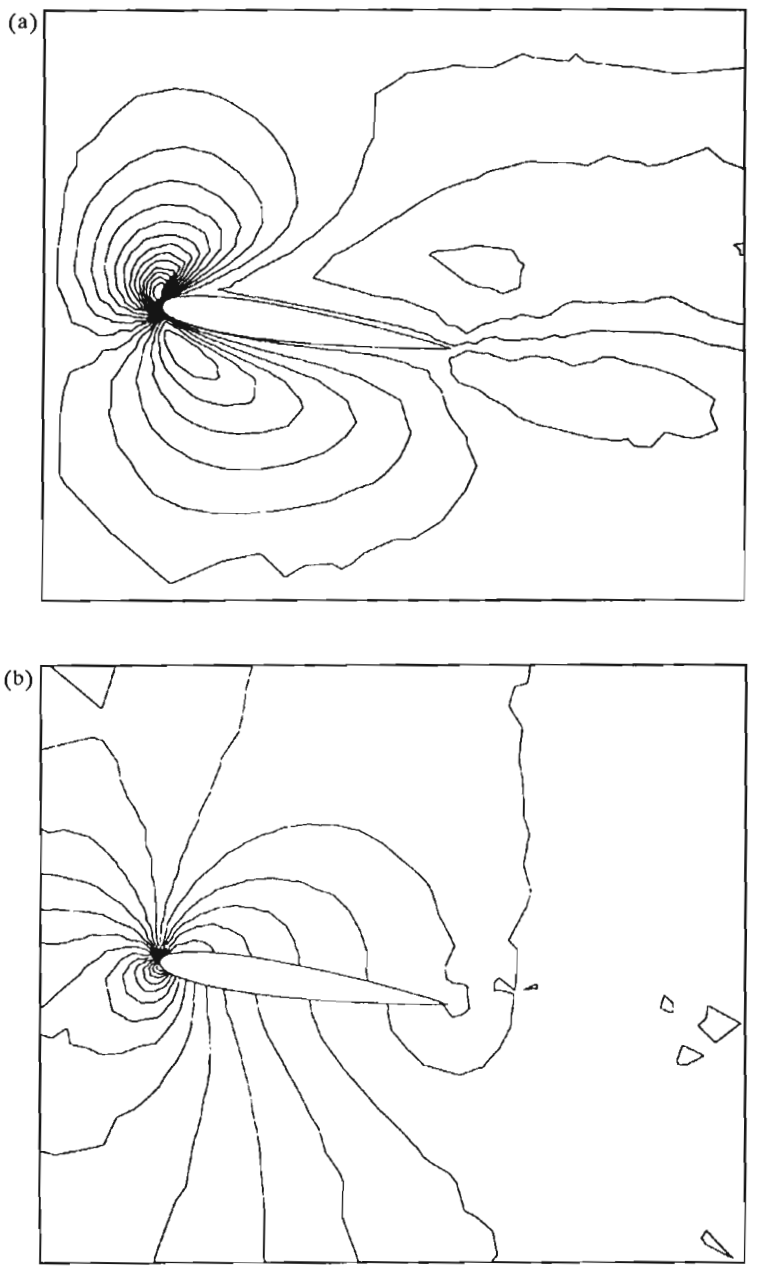

Fig. 5. Flow around airfoil NACA 66-215 $a = 0.6$ with a flap, $\mathrm{Re} = 100$, (a) geometry and an h-adaptive mesh, (b) u_1 velocity component

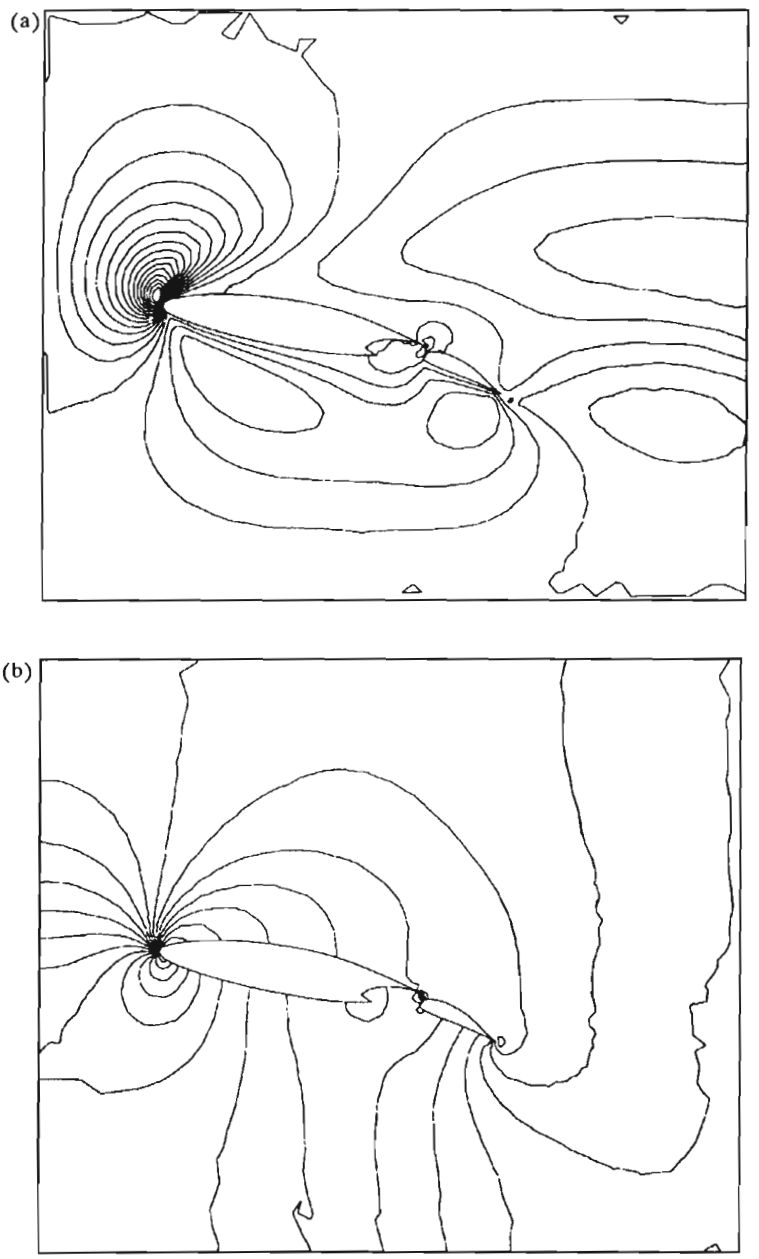

Fig. 6. Flow around airfoil NACA 66-215 $a = 0.6$ with a flap, $\mathrm{Re} = 100$, (a) u_2 velocity component, (b) distribution of pressure

refinements performed with the Rivara algorithm. The solution obtained with the use of "Projection 1" method is shown in Fig.3b and Fig.4. It is characterized with a typical features of such flows: large pressure along the leading edge, the pressure jump across the thickness of the airfoil and the boundary layer.

Example 4: Flow around airfoil NACA 66-215 $a = 0.6$ with a flap

This is a problem of a more complex geometry as shown in Fig.5a. The computational domain was discretized with an unstructured mesh of 1600 linear elements of density increasing around the wing. As in the previous example the Rivara technique was used to generate the adaptive mesh of 3300 elements. The Reynolds number was set to $\mathrm{Re} = 100$. Fig.5b and Fig.6 present the solution. Besides the typical features of the flow we can observe an especially large pressure gradient across the space between the two parts of the wing. A precise resolution of the characteristics of the problem in such a small region was possible because a very fine approximation was introduced automatically by the adaptive procedures.

7. Concluding remarks

In this work we present application of an h-adaptive finite element method to simulations of incompressible viscous flows. The paper is an introductory study of the problem as the range of Raynolds number Re considered was much below the values of Re for realistic engineering applications ($\mathrm{Re} \sim 10^6$).

We report successful numerical experiments with triangular elements of the order $p = 1$ and $p = 2$, and with the Rivara and the 1-irregular meshes techniques of adaptation. Triangular elements seem to be more suitable than quadrilateral elements to discretize domains of complex geometry. On the other hand, quadrilateral elements can be refined directionally allowing for introducing significantly stretched elements which are a necessary tool in discretization of boundary layers, especially for high Reynolds number problems. Combination of these two kinds of approximation seems to be necessary in an efficient Navier-Stokes solver. Another area of the future research is development of the adaptive strategies for transient problems.

Acknowledgment

The support of this work by the State Committee for Scientific Research (KBN) under grant No. 7T07A 010 08 is gratefully acknowledged.

References

1. AINSWORTH M., ODEN J.T., 1993, A Posteriori Error Estimates for Second Order Elliptic Systems: Part 2. An Optimal Order Process for Calculating Self Equilibrating Fluxes, *Comput. Math. Appl.*, **26**, 75-87
2. BABUSKA I., RHEINBOLDT W.C., 1978, Error Estimates for Adaptive Finite Element Computations, *SIAM J. Numer. Anal.*, **15**, 736-754
3. BANK R., SHERMAN R.E., WEISER A., 1983, Refinement Algorithms and Data Structures for Regular Mesh Refinement, *in Scientific Computing*, edit. R.Stepleman et al., IMACS, North Holland
4. BECKER A.J., 1985, *Finite Element Computational Fluid Mechanics*, McGrow-Hill
5. CHORIN A., 1968, Numerical Solutions of the Navier-Stokes Equations, *Math. Comp.*, **82**, 745
6. CHORIN A., 1973, The Numerical Solutions of the Navier-Stokes Equations for an Incompressible Fluid, *Bull. Amer. Math. Soc.*, 73/6, 928
7. DEMKOWICZ L., ODEN J.T., RACHOWICZ W., HARDY O., 1989, Towards a Universal $h-p$ Adaptive Finite Element Strategy, Part 1. Constrained Approximation and Data Structure, *CMAME*, **77**, 79-112
8. GIRAULT V., RAVIART P.A., 1986, *Finite Element Methods for Navier-Stokes Equations*, Springer-Verlag, Berlin Heidelberg
9. GRESHO PH.M., CHAN S.T., 1990, On the Theory of Semi-Implicit Projection Methods for Viscous Incompressible Flow and its Implementation via a Finite Element Method that Introduces a Nearly Consistent Mass Matrix, *Int. Journal for Numerical Methods in Fluids*, **11**, 587-660
10. ODEN J.T., 1994, Error Estimation and Control in Computational Fluid Dynamics, *in The Mathematics of Finite Elements and Applications*, J.R. Whiteman, John Wiley and Sons Ltd
11. ODEN J.T., DEMKOWICZ L., LISZKA T., RACHOWICZ W., 1990, $h-p$ Adaptive Finite Element Methods for Compressible and Incompressible Flows, *Computing Systems in Engineering*, **1**, Nos 2-4, 523-534
12. ODEN J.T., KENNON S.R., TWORZYDLO W.W., BASS T.M., BERRY C., 1993, Progress on Adaptive hp Finite Element Methods for the Incompressible Navier-Stokes Equations, *Computational Mechanics*, **11**, 421-432
13. ODEN J.T., LISZKA T., WU W., 1991, An hp Finite Element Method for Incompressible Viscous Flows, *in The Mathematics of Finite Elements with Applications* (edit. by J.R. Whiteman), Academic Press, London
14. ODEN J.T., WU W., AINSWORTH M., 1994, An a Posteriori Error Estimate for Finite Element Approximations of the Navier-Stokes Equations, *CMAME*, **111**, 185-202
15. RACHOWICZ W., 1995, An Overlapping Domain Decomposition Preconditioner for an Anisotropic h-Adaptive Finite Element Method, *Comput. Methods Appl. Mech. Engng.*, **127**, 269-292
16. RIVARA M.C., 1984, Algorithms for Refining Triangular Grids Suitable for Adaptive and Multigrid Techniques, *Int. J. Numer. Methods Eng.*, **20**, 745-756

h-Adaptacyjna metoda elementów skończonych dla równań Naviera-Stokesa

Streszczenie

W pracy przedstawiono zastosowanie adaptacyjnej metody elementów skończonych do równań Naviera-Stokesa dla dwuwymiarowych przepływów nieściśliwych. Zadanie zdyskretyzowano w czasie stosując metodę projekcji A.Chorina (metodę poprawek ciśnienia). Elementy trójkątne stopnia $p = 1$ i $p = 2$ zostały użyte do dyskretyzacji przestrzennej. Do tworzenia siatek adaptacyjnych zastosowano metodę Rivary i metodę siatek 1-nieregularnych. Strategia adaptacji siatek wykorzystuje rozkład wskaźników błędu obliczanych metodą Odena, Wu i Ainswortha (1994).

Manuscript received October 4, 1996; accepted for print December 2, 1996